Evolution of the Spin Susceptibility of High-T_c Superconductors.

J. Hwang[1],* T. Timusk[1,2], E. Schachinger[3], and J. P. Carbotte[1,2]
[1] *Department of Physics and Astronomy, McMaster University, Hamilton, ON L8S 4M1, Canada*
[2] *The Canadian Institute of Advanced Research, Toronto, Ontario M5G 1Z8, Canada*
[3] *Institute of Theoretical and Computational Physics, Graz University of Technology, A-8010 Graz, Austria*

(Dated: February 6, 2008)

We demonstrate that a new tool, a model independent numerical Eliashberg inversion of the optical self-energy, based on maximum entropy considerations can be used to extract the magnetic excitation spectra of high-transition-temperature superconductors. In $Bi_2Sr_2CaCu_2O_{8+\delta}$ we explicitly show that the magnetic mode that dominates the self-energy at low temperatures directly evolves out of a smooth transfer of spectral weight to the mode from the continuum just above it. This redistribution starts already at 200 K in optimally doped materials but is much weaker in overdoped samples. This provides evidence for the magnetic origin of the superconductivity and presents a challenge to theories of the spin susceptibility and to neutron scattering experiments in high-temperature superconductors.

PACS numbers: 74.25.Gz, 74.62.Dh, 74.72.Hs

The phenomenon of high-temperature superconductivity, discovered in the copper oxides twenty years ago [1], continues to challenge both theorists and experimentalists. From the beginning it was clear that magnetism was an important part of the solution to this puzzle. In conventional superconductors the spectrum of pairing excitation was successfully extracted as an electron-phonon spectral function using an inversion of experimental tunnelling [2] and optical data [3] based on the Eliashberg equation. In principle this spectrum contains the information on the microscopic interactions among electrons mediated by boson exchanges which are needed to describe the superconductivity and can be calculated from band structure information [4]. The primary tools used to map out the magnetic excitations in high-temperature superconductors have been neutron scattering and nuclear magnetic resonance. The picture that has emerged from these studies is a not-well-understood spectrum of excitation dominated by a continuous background extending to unusually high energies, sometimes called the Millis-Monien-Pines (MMP) spectrum [5, 6, 7, 8, 9] which evolves into a broad peak in the local (q integrated) susceptibility at low temperature along with a sharp resonance in the superconducting state centered at $\mathbf{q} = (\pi, \pi)$, the 41 meV mode, named after its frequency in optimally doped $YBa_2Cu_3O_{6+\delta}$ (Y-123) [10, 11, 12, 13, 14, 15]. This sharp resonance has also been seen in $Tl_2Ba_2CuO_{6+\delta}$ [16] and in $Bi_2Sr_2CaCu_2O_{8+\delta}$ (Bi-2212) [17, 18]. The magnetic resonance [6, 19, 20, 21, 22] mode, phonons [23, 24, 25] and the broad continuum [7, 26, 27, 28] in the bosonic spectra have been proposed as candidates for the pairing glue in the copper oxides. Here we use a broader definition of the magnetic resonance as the peak that develops in the local magnetic susceptibility at low temperature. Some theories of the spin susceptibility have predicted that the magnetic resonance develops out of the MMP continuum [6, 29] when the superconducting gap forms. However, so far no consensus has been achieved. To throw new light on this issue we have undertaken a study of the spectrum of excitations responsible for the self-energy of the carriers as a function of temperature and doping in three Bi-2212 systems using optical spectroscopy focussing on the overdoped region of the phase diagram. We clearly observe experimentally for the first time the evolution of a strong peak in the integrated magnetic response developing from the MMP continuum just above it as a function of both *temperature* and *doping*.

The optical self-energy, $\Sigma^{op}(\omega)$ which involves a momentum average, is closely related to the quasiparticle self-energy measured by angle resolved photoemission spectroscopy which is momentum specific. The optical self-energy is is defined in terms of an extended Drude formula [26]:

$$\sigma(\omega) \equiv \frac{i}{4\pi} \frac{\omega_p^2}{\omega - 2\Sigma^{op}(\omega)}, \tag{1}$$

where ω_p is the plasma frequency and $\Sigma^{op}(\omega) \equiv \Sigma_1^{op}(\omega) + i\Sigma_2^{op}(\omega)$. The optical scattering rate is defined by $1/\tau^{op}(\omega) \equiv -2\Sigma_2^{op}(\omega)$. The optical conductivity, $\sigma(\omega)$ can be found through Kramers-Kronig transformation of the reflectance which is measured directly. The numerical inversion of the optical scattering rate is based on an Eliashberg formalism. We start with a deconvolution of the approximate relation [30, 31],

$$\frac{1}{\tau^{op}(\omega;T)} = \int_0^\infty d\Omega K(\omega,\Omega;T) I^2\chi(\Omega), \tag{2}$$

where T is temperature, $K(\omega,\Omega;T)$ is a kernel determined from theory, and $I^2\chi(\Omega)$ is the bosonic spectrum. For the deconvolution we utilized the maximum entropy method, originated by E. T. Jaynes [32]. For the kernel

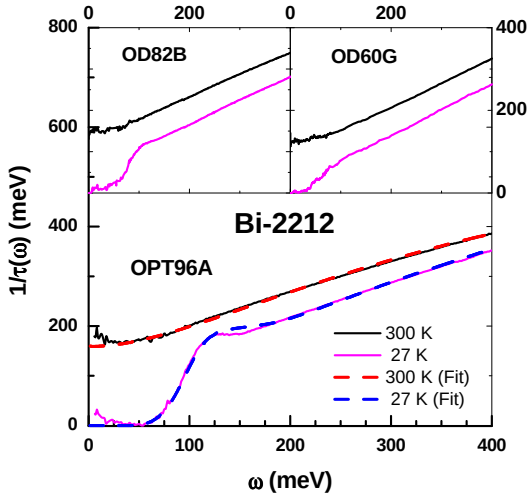

FIG. 1: Optical scattering rate, $1/\tau(\omega)$ as a function of ω. Solid lines are data and dashed lines the Eliashberg fit. Heavy line is for temperature of 300 K (normal) and light for 27 K (superconducting) for optimally doped Bi-2212. In the inset we display the optical scattering rate of our two overdoped samples. They show no low frequency localization effects.

we use [30]:

$$K(\omega,\Omega;T) = \frac{\pi}{\omega}\Big[2\omega\coth(\Omega/2T) - (\omega+\Omega) \times \coth((\omega+\Omega)/2T) + (\omega-\Omega)\coth((\omega-\Omega)/2T)\Big] \quad (3)$$

for the normal state and

$$K(\omega,\Omega;T=0) = \frac{2\pi}{\omega}\Big\langle(\omega-\Omega)\theta(\omega+2\Delta_0(\vartheta)-\Omega) \times E(\sqrt{1-4\Delta_0^2(\vartheta)/(\omega-\Omega)^2})\Big\rangle_\vartheta \quad (4)$$

for the superconducting state where $\langle\cdots\rangle_\vartheta$ denotes the angular average over ϑ and $E(x)$ is the complete elliptic integral of the second order. Here $\Delta_0(\vartheta) = \Delta_0\cos(2\vartheta)$ reflecting the d-wave symmetry of the superconducting order parameter. For the superconducting state at finite temperature we adjust the size of the maximum gap, Δ_0 according to a BCS temperature variation. After small adjustments using full Eliashberg formalism and a least squares fit, we obtain the electron-boson spectral density, $I^2\chi(\omega)$. Details about uniqueness and quality of the fit are described in the literature [30].

We used the self-energy data of Bi-2212 from a previous study [26] on an optimally doped and two overdoped samples. We note that the optimally doped sample is yttrium-doped and somewhat different from conventional optimally doped Bi-2212 having a more ordered structure and a higher T_c. Underdoped systems show pseudogap behavior not yet incorporated in the inversion formalism and are not treated here. In Fig. 1 we show our fit (dashed lines) to data (solid lines) as an example for our

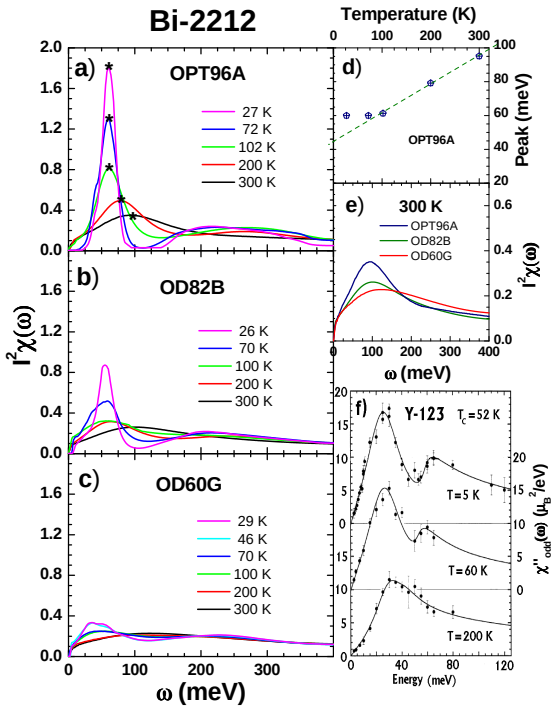

FIG. 2: The bosonic spectra, $I^2\chi(\omega)$, of $Bi_2Sr_2CaCu_2O_{8+\delta}$. (a - c) The doping and temperature dependent bosonic function for three doping levels (T_c = 96 K (OPT), 82 K (OD), and 60 K (OD)). At room temperature all samples exhibit a broad continuum background shown in panel e. On lowering the temperature the broad background peak evolves into a broad peak with a deep valley above it. The spectral weight gained in the peak is roughly balanced by the spectral weight loss in the valley (see Fig. 3b). With increasing doping the intensity of the peak and valley are significantly weakened (see Fig. 3b). Panel d shows the temperature dependence of the frequency of the peak maximum in OPT96A marked by a star. Panel f shows the local magnetic susceptibility of underdoped Y-123 from neutron scattering [5, 8, 33]. While this is a different copper oxide from the ones given in panels a, b and c we note the qualitative similar temperature evolution of panel a.

optimally doped sample OPT96A at two temperatures: heavy lines are for T=300 K (normal) and light lines for T=27 K (superconducting). The fits are very good except for two small spectral regions near zero energy for both states and near the overshoot region for the superconducting state. Above 125 meV in the superconducting state the theoretical curve is flat while the data show a slight depression. The discrepancy near zero energy may come from impurity localization which is observed in most cuprate systems. We note that the optimally doped sample shows the strongest localization but this does not affect to the main sharp peak in $I^2\chi(\Omega)$. The two overdoped samples show negligible localization (see the insets in Fig. 1).

In Fig. 2a, b and c we plot the extracted bosonic spectra, $I^2\chi(\omega)$, of Bi-2212. We observe dramatic temperature and doping dependencies. The room temperature spectra show a broad continuum which exhibits some doping dependence as shown in panel e. At lower doping levels the broad peak in the spectrum becomes somewhat stronger and shifts to lower frequencies, which is consistent with a previous neutron study [8] on underdoped $YBa_2Cu_3O_{6.6}$. The temperature and doping dependence, as we move from panel a to panel c, is more striking. On the lowering of the temperature nearly all the spectral weight below 130 meV in the optimally doped material is moved to a resonance peak while in the overdoped region less and less of the continuum spectral weight is transferred to this peak. The peak in the room temperature spectrum, at 97 meV in panel a, shifts continuously to lower energies as its intensity grows. The panel d shows that the peak position is approximately linear in temperature above $T = 100$ K and saturates to 60 meV below this temperature. What is notable about this process is that this evolution takes place through a transfer of spectral weight from frequencies above the peak leaving a valley between 100 to 150 meV. In addition, there is a well developed 30 meV gap on the low frequency side of the peak. Such a gap in the spin susceptibility is consistent with the observations of spin-polarized neutron scattering of optimally doped Y-123 with T_c=91 K [33]. As shown in Fig. 2b and 2c for higher doping levels the gap in the spin susceptibility becomes small and the resonance mode can still be discerned although it weakens significantly [26]. In our most overdoped sample (OD60G) only a small fraction of spectral weight in the bosonic spectrum contributes to the temperature redistribution.

We also show the local (q integrated) magnetic susceptibility, $\chi''_{odd}(\omega)$, from neutron scattering study of underdoped Y-123 [5, 8] in Fig. 2f to compare its temperature dependent spectral weight redistribution with that of the bosonic excitation, $I^2\chi(\omega)$, of our optimally doped Bi-2212 (OPT96A). Although they are different copper oxide systems and at different doping levels they qualitatively contain common temperature dependent features which we described previously. A similar spectral redistribution of the local magnetic susceptibility has been observed by Dai *et al.* [14]. However, it was not widely recognized or confirmed by other experiments. Here we find that the spectral redistribution occurs mainly in the low frequency region below 200 meV and is strongly doping dependent on the overdoped side of the phase diagram.

Alternatively, we can look at the spectrum at low temperature in panel a of Fig. 2 as the development of a large 130 meV gap in the spin fluctuation spectrum with a mode in the middle of the gap at 60 meV. Such a transformation has been considered by Abanov and Chubukov [6] but with the gap arising at $2\Delta_0$ with Δ_0 the superconducting gap. Here we find a much larger gap that starts to form already at $T = 200$ K, well above T_c.

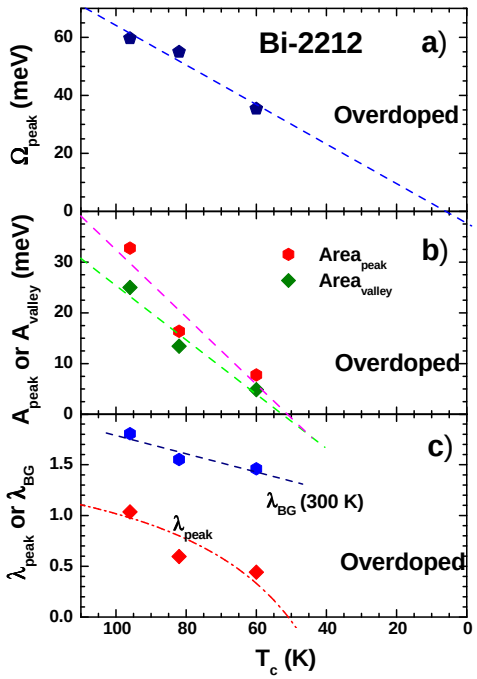

FIG. 3: T_c dependent properties of the peak and the valley (see in the text). a) The central peak frequency is proportional to T_c, i.e., $\Omega_{peak} = 8.0k_BT_c$, and the dashed line is a linearly fitted line. b) The peak and valley are closely connected, have a very similar T_c dependence and vanish at the same $T_c \approx 50$ K. The dashed lines are linearly fitted lines. c) The coupling constant, λ_{peak}, vanishes at the same T_c as the peak and valley. The coupling constant, λ_{BG}, of the continuous background shows a weaker T_c dependence as compared to that of the peak. The dash-dotted line is obtained by using the linearly fitted center frequency (Fig. 3a) and area under the peak (Fig. 3b), i.e., $\lambda_{peak} \simeq 2A_{peak}/\Omega_{peak}$.

To study quantitatively the changes in the bosonic spectra we subtract the room temperature spectrum from the lower temperature spectra. We clearly observe a peak and a valley in the difference spectra. In Fig. 3 we display the T_c dependence of the peak and valley in the bosonic spectra. Fig. 3a shows the center frequency of the peak, Ω_{peak} versus T_c at our lowest measured temperatures. We find $\Omega_{peak} \approx 8.0k_BT_c$, which is similar to the temperature dependence of the magnetic resonance mode ($\Omega_{res} \approx 5.3k_BT_c$). In Fig. 3b we plot the the area under the peak and of the valley above it as a function of the critical temperature for our lowest temperature (for the optimally doped we also include the 30 meV gap as part of the valley). The two areas show the same trend; both decrease rapidly as T_c decreases in the overdoped region and their extrapolation show that they vanish at the same T_c near 50 K. The total spectral weight up to 400 meV is conserved to within 15 % which indicates a small frequency dependence of the coupling constant I^2 in $I^2\chi(\Omega)$. We also calculate the T_c dependent cou-

pling constant, $\lambda(T_c) = 2\int_0^{\omega_c} I^2\chi(\Omega)/\Omega d\Omega$, using only the peak ($\lambda_{peak}$) or the continuum ($\lambda_{BG}$) for $I^2\chi(\Omega)$. Here ω_c is a cutoff frequency, taken as 400 meV. These are shown in Fig. 3c. The peak coupling constant λ_{peak} decreases rapidly extrapolating to zero at T_c =50 K. The coupling constant of the background λ_{BG} shows a weaker dependence on T_c.

Our novel analysis of the optical data has provided new and detailed information on the redistribution with temperature and doping levels of the spectral weight in the inelastic scattering spectral function. This analysis of optical data, based on an Eliashberg inversion, is the only existing method to date which can be used to study the evolution of the spin susceptibility as a function of doping and temperature across the phase diagram of high-T_c oxides. Furthermore this analysis can also be applied to other existing optical spectra to get new information on their excitation spectrum. Our central new finding is that the optical resonance peak which becomes prominent at low temperature in our optimally doped sample, forms mainly through the transfer of spectral weight from the energy region immediately above it. This constitute strong evidence that the peak and background in the bosonic spectral function have the same microscopic origin. Identifying the optical peak with the resonance in the local magnetic susceptibility measured by neutron scattering, we conclude that the background which dominates the inelastic interaction at and above T_c is magnetic in origin.

Finally we note that we have also identified a new temperature scale, around 200 K in the optimally doped Bi-2212, where the magnetic fluctuation spectrum begins to soften and develop the peak in the local magnetic susceptibility. To our knowledge current theories do not account for this phenomenon.

This work has been supported by the Canadian Natural Science and Engineering Research Council and the Canadian Institute of Advanced Research. We acknowledge the contribution of Genda Gu and Hiroshi Eisaki in growing the crystals that we used. We have profited from discussions with Philip Anderson, Philip Bourges, Andrey Chubukov, Matthias Eschrig, Berhnard Keimer and Chandra Varma.

* Electronic address: hwangjs@mcmaster.ca

[1] T. G. Bednorz, K. A. Müller, Z. Phys. B **64**, 189 (1986).
[2] J. P. Carbotte, Rev. Mod. Phys. **62**, 1027 (1990).
[3] B. Farnworth, T. Timusk, Phys. Rev. B **10**, 2799 (1974); *ibid.* Phys. Rev. B **14**, 5119 (1976).
[4] P. G. Tomlinson, J. P. Carbotte, Phys. Rev. B **13**, 4738 (1976).
[5] P. Bourges, H. F. Fong, L.P. Regnault, J. Bossy, C. Vettier, D. L. Milius, I. A. Aksay and B. Keimer, Phys. Rev. B **56**, R11439 (1997).
[6] Ar. Abanov, A. V. Chubukov, Phys. Rev. Lett. **83**, 1652 (1999).
[7] A. J. Millis, H. Monien, D. Pines, Phys. Rev. B **42**, 167 (1990).
[8] H. F. Fong, P. Bourges, Y. Sidis, L.P. Regnault, J. Bossy, A. Ivanov, D. L. Milius, I. A. Aksay and B. Keimer, Phys. Rev. B **61**, 14773 (2000).
[9] V. Hinkov, P. Bourges, S. Pailhes, Y. Sidis, A. Ivanov, C. T. Lin, D. P. Chen and B. Keimer, e-print, cond-mat/0601048 (2006).
[10] J. Rossat-Mignod, L. P. Regnault, C. Vettier, P. Bourges, P. Burlet, J. Bossy, J. Y. Henry and G. Lapertout, Physica C **185-189**, 86 (1991).
[11] H. A. Mook, M. Yethiraj, G. Aeppli, T. E. Mason and T. Armstrong, Phys. Rev. Lett. **70**, 3490 (1993).
[12] H. F. Fong, B. Keimer, P. W. Anderson, D. Reznik, F. Dogan and I. A. Aksay, Phys. Rev. Lett. **75**, 316 (1995).
[13] H. A. Mook, P. Dai, S. M. Hayden, G. Aeppli, T. G. Perring and F. Dogan, Nature **395**, 580 (1998).
[14] P. Dai, H. A. Mook, S. M. Hayden, G. Aeppli, T. G. Perring, R. D. Hunt and F. Dogan, Science **284**, 1344 (1999).
[15] M. Eschrig, Adv. in Phys. **55**, 47-184 (2006).
[16] H. He, P. Bourges, Y. Sidis, C. Ulrich, L. P. Regnault, S. Pailhs, N. S. Berzigiarova, N. N. Kolesnikov and B. Keimer, Science **295**, 1045 (2002).
[17] H. F. Fong, P. Bourges, Y. Sidis, L. P. Regnault, A. Ivanov, G. D. Gu, N. Koshizuka and B. Keimer, Nature **398**, 588 (1999).
[18] H. He, Y. Sidis, P. Bourges, G. D. Gu, A. Ivanov, N. Koshizuka, B. Liang, C. T. Lin, L. P. Regnault, E. Schoenherr and B. Keimer, Phys. Rev. Lett. **86**, 1610 (2001).
[19] M. R. Norman, H. Ding, Phys. Rev. B **57**, R11089 (1998).
[20] J. C. Campuzano *et al.*, Phys. Rev. Lett. **83**, 3709 (1999).
[21] J. F. Zasadzinski, L. Ozyuzer, L. Coffey, K. E. Gray, D. G. Hinks and C. Kendziora, Phys. Rev. Lett. **96**, 017004 (2006).
[22] K. Terashima, H. Matsui, D. Hashimoto, T. Sato, T. Takahashi, H. Ding, T. Yamamoto and K. Kadowaki, Nature Physics, **2**, 27 (2006).
[23] A. Lanzara, P. V. Bogdanov, X. J. Zhou, S. A. Kellar, D. L. Feng, E. D. Lu, T. Yoshida, H. Eisaki, A. Fujimori, K. Kishio, J.-I. Shimoyama, T. Noda, S. Uchida, Z. Hussain and Z.-X. Shen, Nature **412**, 510 (2001).
[24] G.-H. Gweon, T. Sasagawa, S. Y. Zhou, J. Graf, H. Takagi, D.-H. Lee and A. Lanzara, Nature **430**, 187 (2004).
[25] X. J. Zhou *et al.*, Phys. Rev. Lett. **95**, 117001 (2005).
[26] J. Hwang, T. Tumsk, D. G. Gu, Nature **427**, 714 (2004).
[27] J. P. Carbotte, E. Schchinger, D. N. Basov, Nature **401**, 354 (1999).
[28] E. Schachinger, J. P. Carbotte, Phys. Rev. B **62**, 9054 (2000).
[29] See for example: D. K. Morr, D. Pines, Phys. Rev. Lett. **81**, 1086 (1998) and references therein.
[30] E. Schachinger, D. Neuber, J. P. Carbotte, Phys. Rev. B **73**, 184507 (2006).
[31] S. V. Dordevic, C. C. Homes, J. J. Tu, T. Valla, M. Strongin, P. D. Johnson, G. D. Gu, and D.N. Basov Phys. Rev. B **71**, 104529 (2005).
[32] E. T. Jaynes, Phys. Rev. **106**, 620 (1957).
[33] P. Bourges *et al. High Temperature Superconductivity* edited by S. E. Barnes *et al.* (CP483 American Institute of Physics, Amsterdam, 1999), 207 (1999).